HYBRID FLYWHEEL (Hy-FLY) ENERGY STORAGE SYSTEM (ESS) FOR OFFSHORE WIND APPLICATION

Nikhil K Mishra[1], Debanjan Mukherjee[2], Karuna Kalita[1*], Seamus D Garvey[3], James P Rouse[3], Prabir Barooah[4]*

[1]*Department of Mechanical Engineering Indian Institute of Technology, Guwahati, India*
[2]*School of Energy Science and Engineering, Indian Institute of Technology, Guwahati, India*
[3]*Faculty of Engineering, University of Nottingham, NG7 2RD, Nottingham, United Kingdom*
[4]*Department of Electrical and Electronics Engineering Indian Institute of Technology, Guwahati, India*
**nikhil1996@iitg.ac.in*
**karuna.kalita@iitg.ac.in*

Keywords: Grid Inertia, Offshore Wind, Hybrid Energy Storage.

Abstract

Several factors have raised interest in discovering low-carbon electricity production sources. Out of all renewable energy (RE) sources, offshore wind is being rapidly integrated into the electrical grid worldwide. Inertia in the grid refers to the energy stored in large rotating turbogenerators and some industrial motors, which gives them the tendency to continue rotating. The kinetic energy of the rotating masses in thermal power plants arrests the fall of frequency. Thus, the traditional power plants' inertia helps to maintain the grid stability by allowing the grid control systems to act after the initial few seconds. This helps in maintaining the frequency within the prescribed range. However, most of the renewable energy-based power generation systems are connected to the grid via a power electronic converter of some description (AC to DC and DC to AC power converters), providing little to no intrinsic inertial response to the varying load generation mismatch of the grid system. As RE systems continue to displace fossil-fuelled generation, significant amounts of real inertia are being lost. Presently this loss of real inertia is compensated by taking measures such as introducing synthetic inertia, inertia emulation etc. The grid operation strategy is also changed so that the largest loss of generation can be controlled. For the stable functioning of any electrical grid, the generation and demand must be in equilibrium without severe variations. Thus, the novelty of this study is to develop a system for providing real inertia, which helps to control the rate of change of frequency (RoCoF) when an overloading event happens in the grid. The system makes use of real inertia as well as a secondary energy store. The concept combines a flywheel (a source of real inertia) and secondary energy stores coupled to a synchronous generator. The flywheel and the secondary energy storage system are connected to the synchronous generator through an electromechanical differential drive unit that enables to take advantage of high-system inertia during the arresting period of RoCoF while allowing the flywheel and secondary storage to extract energy when the system is discharging.

1. Introduction

The rising demand for energy to pursue transportation, industrial, commercial, and economic activities across the globe has led to an overall increase in global energy consumption in terms of renewable and non-renewable energy sources [1]. Vastly available renewable energy resources prove to be a promising solution for satisfying energy demand considerations across all countries in the world because these emit less to no carbon into the atmosphere and can generate energy at a very low cost. The rapid integration of renewable energy sources into the electrical grid will lead to decommissioning or shutdown of traditional thermal power plants in the near future, which provide stability to the grid by providing rotating inertia [2]. In real-time, it is paramount that the electricity demand and generation must be balanced for the stability of the grid [3]. When an overloading event (i.e. generation and demand mismatch) happens in the grid, the immediate result is an instantaneous deviation of the grid frequency. It is the inertia of the grid which limits the rate of change of frequency [3].

The intermittent nature of renewable energy sources creates a significant disadvantage that cannot be ignored during the planning of grid dispatch services. Further, if continuous supply is to be obtained, at least some sort of energy storage is required [4]. The imbalance in generation and demand must be taken into account across all periods ranging from milliseconds to weeks and even months [5]. In traditional power plants, during any short-term imbalance of energy, the inertia of the turbogenerator arrests the rate of change of frequency of the synchronous machine by providing the necessary time to activate the other frequency stabilization services [6]. On the other hand, renewable energy sources have linking power electronic devices that do not provide inertia response to the grid imbalance, unlike the traditional power plants with synchronous generators[7]–[10]. Renewable energy can also be termed inertia-less RE sources. The wind turbine has a small amount of inertia [11]. However, due to the

https://doi.org/10.1049/icp.2023.1591

connected power electronics, it is debatable if the grid actually perceives this inertia. In order to sustain such a load imbalance, grid-scale energy storage systems are built that can be integrated with these on-grid renewable energy systems to provide sufficient inertia and prohibit a tentative grid collapse due to frequency deviation outside the working range.

Energy storage systems can be classified into very short, short, medium, and long durational energy storage systems [12]. Short durational energy storage systems can be grid-scale and can be utilized to provide fast frequency response services during grid overloading events, generally in milliseconds. Flywheel energy storage systems (FESS) fall under this category and can be utilized to provide an inertial response to the grid in a very short time. FESS operation can be described in a way that during the charging process, the electric supply charges the flywheel that stores energy in the form of kinetic energy by speeding up its rotational velocity. This stored kinetic energy is released during application. The amount of stored energy is based on the mass moment of inertia and rotational speed of the flywheel [13]. The FESSs can be classified as high-speed (10,000 – 100,000 rpm) and low-speed (less than 6000 rpm) [14]–[16]. The FESS works completely in a passive manner. The system's resistance to changing its speed determines the transmission of energy entirely. Apart from having the benefits of providing large amounts of inertia, flywheel energy storage systems have long operating and cycle lifespans, high turnaround efficiency, high energy densities, and little adverse environmental impacts [17].

This study proposes an electricity in/ electricity out energy storage system that bridges the gap between different energy storage time scales. We refer to this system as hybrid flywheel Energy Storage (Hy-FLY). The sudden generation-load anomalies have been addressed through the introduction of real inertia by a flywheel and the continuous supply of energy for the longer period is addressed through secondary energy reserves. The secondary energy sources can be compressed air energy storage systems (CAES) or battery energy storage systems (BESS). Here, a 50MW system with a 20MWh capacity has been proposed with the idea that this design may contribute to the energy storage needs of an offshore wind farm.

In literature, flywheel-based hybrid energy storage systems have been proposed with a focus on renewable energy sources, particularly wind energy (for examples, see the work of Prodromidis and Coutelieris [18], [19] and Sebastián and Pea-Alzola [20]). Of particular interest here is the publication where a synchronous machine was attached to a flywheel using a hydraulic transmission linking the two components [17]. Building on this work, an epicyclic gear based electromechanical differential drive unit (DDU) is proposed, which connects the primary synchronous generator with a flywheel and a secondary motor which is powered by a secondary energy source (i.e. compressed air). This DDU allows to transfer energy from the flywheel and secondary source to the primary synchronous generator while spinning at different speeds. The constant speed of the primary synchronous generator is maintained with the help of the secondary motor during different modes of operations. Moreover, the proposed Hy-FLY system provides a solid link between the main source of inertia (flywheel) and the synchronous generator. This also overcomes the potentially significant losses associated with hydraulic transmission proposed in the DDU in [17].

In the proposed hybrid flywheel energy storage system, the voltage regulation electronics are used, which are also part of the traditional synchronous machine of thermal power plants. In general, it was found that synchronous machines performed better for demand load variations, and variable speed configurations (asynchronous machines) performed better for accommodating wind speed variations. The synchronous system here still shows the advantages of matching demand variations.

2. Hybrid flywheel Energy Storage (Hy-FLY)

A hybrid energy storage system is distinguished by the addition of two or more energy storage technologies with the additional operational properties (such as energy and power density, self-discharge rate, efficiency, lifetime, etc.). One energy store in a hybrid energy storage system is often devoted to handling "high power" demand, transients, and quick load variations. It is characterised by a quick response time, high efficiency, and long cycle lifetime. The other energy store will be "high energy" storage with a low self-discharge rate and reduced energy-specific installation costs [21].

The proposed hybrid system is a series type system that is completely different from the majority of the design proposed in literature called parallel type system, where several energy storage technologies feed a common bus, and each storage requires an individual controller to react to the grid imbalance [21]–[23]. Hy-FLY has a single primary synchronous generator (per base unit) connected to the grid that produces power in a synchronous manner, thereby removing the need for power converter electronics and work similar to a traditional synchronous power generator. Additionally, the proposed system enables energy to be simultaneously stored and withdrawn from two different sources at rates suitable for a particular grid situation.

The short-term quick response demand is supported by spinning down the flywheel. For the prolonged energy demand, the synchronous generator will run at synchronous speed while extracting energy from the flywheel and secondary energy storage (compressed air). As the flywheel spins down, there would be a distinct decrease in the power ratio between the flywheel and the secondary energy storage.
An overview of Hy-FLY is shown in Figure 1. The hybrid flywheel energy storage system comprises an epicyclic gear-based electromechanical differential drive unit DDU, a primary synchronous machine connected to DDU through a solid rigid shaft, a secondary synchronous machine connected to DDU powered by secondary energy stores, and a flywheel connected to the DDU through a solid rigid shaft. The DDU allows a slip between the speed of the primary synchronous

generator rotor and flywheel. The power from the secondary energy stores depends on the amount of slip. A clutch is placed between the flywheel and DDU to disconnect the flywheel once 80% of the stored energy from the flywheel is extracted. A 2-pole machine is favoured over a 4-pole synchronous machine. The advantage of a 2-pole design over a 4-pole type is that 2-pole machines have double the synchronous speed of 4-pole machines.

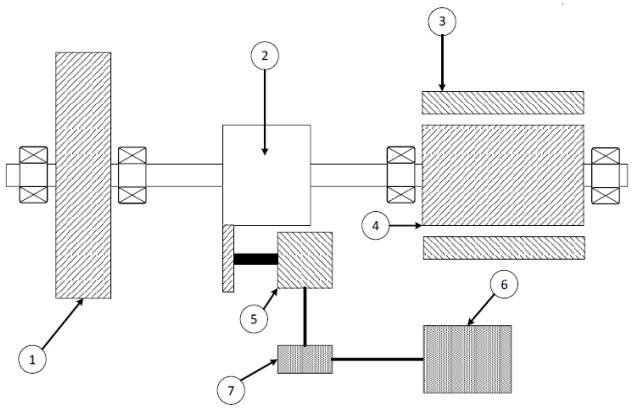

Figure 1: The proposed hybrid flywheel energy storage system (Hy-FLY).

(1) Flywheel
(2) Electromechanical differential drive unit
(3) Primary synchronous machine stator
(4) Primary synchronous machine rotor
(5) Secondary synchronous machine
(6) Secondary energy storage
(7) Controller for secondary synchronous machine

In the flowchart shown in Figure 2, the various operating modes of Hy-FLY are described. Assume Hy-FLY is operating in mode 1, where the DDU is locked acting as a direct drive, and the rotor shaft of the primary synchronous machine and shaft of the flywheel act as a single shaft. The primary synchronous machine rotor and flywheel both revolve at the same speed ($\omega_{SM} = \omega_{FW}$ where ω_{FW} and ω_{SM} are the respective rotational speeds of the flywheel and primary synchronous machine respectively). Let us assume that the speed is synchronous (100π rad/s for a two-pole machine), and the system is initially unloaded. When an overloading event occurs, the system starts discharging by slowing down the flywheel speed. The primary synchronous machine will act as a generator. Initially, in mode 1, the system is locked; therefore, the system has both flywheel and rotor inertia. Upon discharging, the speed of the synchronous machine decreases to the lower limit of synchronous speed ω_{SMLL} (with this being the minimum speed at which the synchronous machine can run so that the generated frequency is within the grid acceptance limit). It is to be noted that in India, as per the Indian Electricity Grid Code (IEGC) 2010, all users and State Load Despatch Centre (SLDC) should use all reasonable efforts to maintain the grid frequency within the range of 49.5 to 50.5 Hz at all-time [24]. Once the lower limit of synchronous speed is reached, the DDU is unlocked (this is mode 2A during discharge), allowing the flywheel and synchronous machine to rotate at different speeds. As the mode 2A is activated, the secondary energy storage (secondary synchronous machine powered by compressed air) comes into action so that a constant torque is maintained over DDU through a control mechanism, thus extracting energy from the flywheel by slowing it down and restoring the rotor speed back to nominal synchronous speed ($\widetilde{\omega}_{SM}$) with the help of the secondary energy storage.

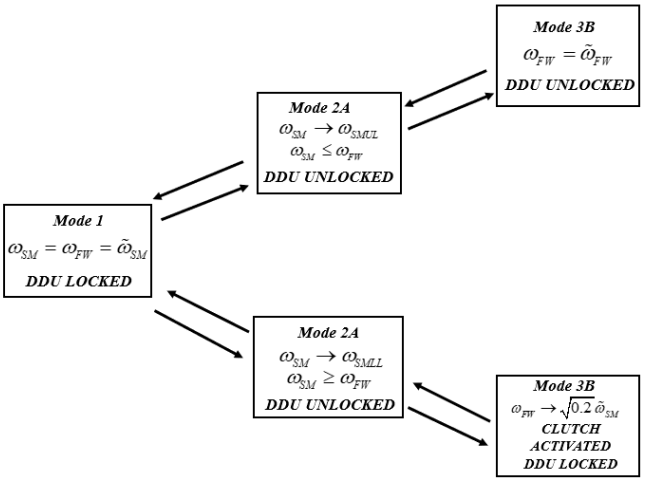

Figure 2: Hy-FLY operating mode flowchart

The control of the secondary synchronous machine connected to DDU, which determines the frequency of the primary synchronous machine, is achieved by comparing the (ω_{SM}) to ($\widetilde{\omega}_{SM}$). The minimum flywheel speed cannot be near zero because the needed torque for low speed would be too high; therefore, the Hy-FLY flywheel is disconnected from the system using a clutch once the 80% of the energy stored in the flywheel is extracted (when the $\omega_{min} = \sqrt{0.2}\omega_{max}$ 80% energy is extracted) the system is again locked mode 3A.

During charging mode, (from the system in mode 3A), the clutch is engaged, and the DDU is unlocked. A negative torque is applied by the DDU on the primary synchronous machine as it tries to slow it down whilst a positive torque is applied on the flywheel which increases its speed. Once the speed of the flywheel reaches to nominal synchronous speed ($\widetilde{\omega}_{SM}$), the system moves to mode 1, and DDU gets locked. The primary synchronous machine rotor shaft and flywheel shaft become locked together, locking the DDU. The speed of the flywheel is further increased to the upper tolerance speed of the synchronous machine (ω_{SMUL}) in mode 2B (ω_{SMUL}, which is the maximum speed at which the synchronous machine will run so that the generated frequency lies within the grid acceptance limit).

The speed of the flywheel can further increase from here to its upper limit ($\widetilde{\omega}_{FW}$) by unlocking the system in order to store more energy (mode 3B). It should be noted that there is the structural limit of the material, which prohibits it from spinning up.

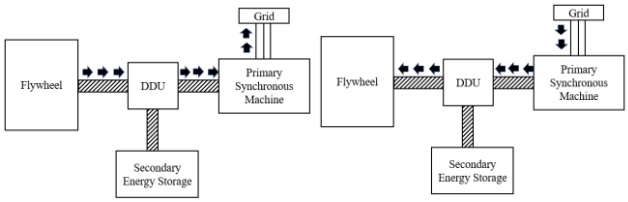

Decreasing grid frequency Increasing grid frequency

Figure 3: Power flow when DDU is locked in mode 1

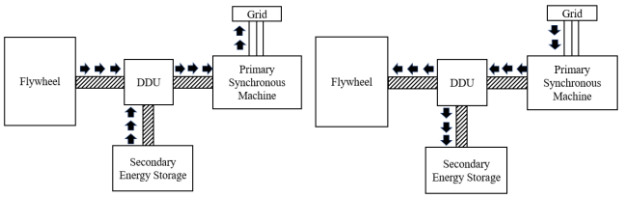

System discharging System charging

Figure 4: Power flow when DDU is unlocked in modes 2 and 3

3. Hy-FLY basic design calculation

High-power designs play a crucial role in providing a significant impact on the energy market. Thus, the present work focuses on developing a 50 MW (20 MWh capacity) system which is similar and comparable to a hydro-storage system [25] and would enhance the applications of offshore wind generators**.** The work describes the calculations for the fundamental sizing of a 50 MW Hy-FLY system. The kinetic energy in the flywheel is proportional to the square of its rotational velocity and the mass moment of inertia of the flywheel. It is given by Equation (1).

$$E_K = \frac{1}{2} J_{FW} \omega^2 \tag{1}$$

$$J_{FW} = \frac{1}{2} \times m \times (r_0^2 - r_i^2) \tag{2}$$

where E_K is the kinetic energy stored in the flywheel, J_{FW} is the mass moment of inertia of the flywheel, ω is the rotational velocity of the flywheel, m is the mass of the flywheel and $\frac{r_0}{r_i}$ are the external and internal bore radius of the flywheel, respectively. A 2-pole synchronous machine is considered over a 4-pole design here as explained in the section 2, giving rise to a synchronous rotational velocity of 100π rad/s ($\omega_{SM} = \frac{4\pi f}{p}$ where f is the nominal frequency of the synchronous machine and p is the number of poles of the machine). The amount of energy held or released by the flywheel is given by Equation (3).

$$\Delta E_K = \frac{1}{2} J_{FW} (\omega_{max}^2 - \omega_{mix}^2) \tag{3}$$

where the flywheel's maximum and minimum rotational velocities are represented by ω_{max} and ω_{min} respectively. The minimum flywheel speed cannot be close to zero since the required torque to speed up the huge mass of flywheel from such a low speed would be very high.[19], [26]. Therefore, the flywheel minimum speed is considered to be ($\omega_{min} = \sqrt{0.2}\,\omega_{max}$ where 80% energy stored in the flywheel is extracted). Using Equation (3) it can be found that the flywheel of a storage capacity of 20 MWh will require a mass moment of inertia of $J_{FW} = 1.823 \times 10^6 kg.m^2$considering $\omega_{max} = 100\pi$ for a 2-pole machine.

The kinetic energy store in the rotor of the synchronous machine can be calculated from the inertia constant H and the base rating of the machine B as shown in Equation (4)[26]. Units of H, B are in MJ/MVA and MVA respectively. Assuming $H = 6\frac{MJ}{MVA}$ (which is a characteristic of a condensing turbine generator) and using Equation (1) the basic definition of kinetic energy and Equation (4) the moment of inertia of synchronous machine is found to be $J_{SM} = 6.079 \times 10^3 kg.m^2$.(which is a characteristic of a condensing turbine generator) and using Equation (1) the basic definition of kinetic energy and Equation (4) the moment of inertia of synchronous machine is found to be $J_{SM} = 6.079 \times 10^3 kg.m^2$.

$$(E_K)_{SYN} = BH \tag{4}$$

Setting a burst speed determines the flywheel mass (in terms of utilisation of resources and packaging). The accurate knowledge of the stress distribution is necessary to design the burst speed of the flywheel. The Tresca yield criteria have long been associated with the solution to the stress and deformation within a thin rotating elastic plastic disc [27]. Nadai [28]noted that radial and hoop stresses are found to be sufficiently accurate when the thickness is small when compared to the diameter. The flywheel disk thickness is considered to be sufficiently small to assume the plane stress state condition. Hence, the design calculation of the flywheel is based on the constant thickness thin rotating hollow disk of an elastic-perfectly-plastic (EPP) material in relation to the Tresca yield criterion. The design procedure is well documented in [29]. Tresca yield criterion indicates that the limiting case (burst), i.e. when material yielded throughout the entire radius of the flywheel, occurs when $\sigma_y = \sigma_\theta$ (where, σ_y= Yield strength, σ_θ= Hoop stress) for all r (radial coordinate). Equation (5) describes the equilibrium condition for a rotating disk. Substituting $\sigma_y = \sigma_\theta$ in Equation (5) and subsequently, integrating it generates Equation (6). In Equation (6), constant A is determined using the boundary condition as at $r = r_i$ (inner radius) radial stress is zero ($\sigma_r = 0$). This gives the radial stress distribution represented by Equation (7).

$$\sigma_\theta - \sigma_r - r\frac{d\sigma_r}{dr} = \rho r^2 \omega^2 \tag{5}$$

$$\sigma_r = \sigma_y - \frac{\rho r^2 \omega^2}{3} + \frac{A}{r} \tag{6}$$

$$\sigma_r = \sigma_y \left(1 - \frac{r_i}{r}\right) - \left(\frac{\rho\omega^2}{3}\right)\left(r^2 - \frac{r_i^3}{r}\right) \tag{7}$$

3.1 Flywheel design calculation for 50 MW (20 MWh capacity systems):

The internal bore radius is calculated based on the size of the shaft required to transmit the rated power (50MW), which indicates that $r_i = 0.1m$. The outer radius is calculated at design speed considering that at $r = r_0$, the radial stress is zero($\sigma_r = 0$). Using EN24 steel, which has a yield strength of $\sigma_y = 940$MPa, and mass density $\rho = 8170\,\frac{kg}{m^3}$ [30]as flywheel material it is found that $r_0 = 1.647m$. The design speed (ω_D) is taken to be 1.1 times the nominal synchronous speed of the machine ($\widetilde{\omega}_{SM}$) such that a completely plastic flywheel is not realised at nominal operating speed which is ($\widetilde{\omega}_{SM}$). Since, Tresca criterion is fairly conservative, the design speed (ω_D) needs to be slightly higher than the maximum flywheel operational speed ($\widetilde{\omega}_{SM}$). Fully plastic flywheel stress distribution (i.e. when$\omega = \omega_D$) can be seen in Figure 3. The mass of the flywheel m, is calculated from Equation (2) as $1.349 \times 10^6 kg$ and the length of the flywheel (L) is also calculated as $19.29m$. The casting of the flywheel of the size specified in this article as a single unit is anticipated to provide several difficulties while manufacturing and transportation. The flywheel in the current study is therefore anticipated to be composed of a number of laminations restricted axially. The plane stress condition is thus presumed to be true in this instance.

At lower speeds (*i.e.* when $\omega \leq \omega_D$), the flywheel material yields to an intermediate radius r_{ep} while the outer portion remains elastic. The two-zone is treated separately to find the radial and hoop stress distributions. For the outer elastic zone (where $r_{ep} \leq r \leq r_o$) the radial and hoop stress is given by Lame's thick-walled cylinder equation modified with a centrifugal stress term [31]. Considering each disc, the stresses developed in the elastic zones are given by Equations (8) and (9).

$$\sigma_r = A - \frac{B}{r} - \frac{(3+\nu)\rho\omega^2 r^2}{8} \tag{8}$$

$$\sigma_\theta = A + \frac{B}{r} - \frac{(1+3\nu)\rho\omega^2 r^2}{8} \tag{9}$$

where A and B are constant ($\nu$is Poisson ratio of the material), and they may be found from conditions (a) at $r = r_0$ (outer radius) the radial stress is zero$\sigma_r = 0$ and (b) at $r = r_{ep}$ (plastic to elastic transition radius) the hoop stress is equal to yield strength ($\sigma_\theta = \sigma_y$), which gives Equations (10) and (11).

$$\frac{B}{\sigma_y} = \frac{[1 - (\rho\omega^2/8\sigma_y)\{(3+\nu)r_o^2 - (1+3\nu)r_{ep}^2\}]r_o^2 r_{ep}^2}{r_{ep}^2 + r_o^2} \tag{10}$$

$$\frac{A}{\sigma_y} = \frac{[1 - (\rho\omega^2/8\sigma_y)\{(3+\nu)r_o^2 - (1+3\nu)r_{ep}^2\}]r_o^2 r_{ep}^2}{r_{ep}^2 + r_o^2} + \frac{(3+\nu)\rho\omega^2 r_o^2}{8\sigma_y} \tag{11}$$

Finally, r_{ep} may be found by ensuring the continuity in $\sigma_r$within both zones at r_{ep}which gives Equation (12) (For the continuity at r_{ep} equating Equation (7) and (8)).

$$\sigma_y\left(1 - \frac{r_i}{r_{ep}}\right) - \left(\frac{\rho\omega^2}{3}\right)\left(r_{ep}^2 - \frac{r_i^3}{r_{ep}}\right) = A - \frac{B}{r_{ep}} - \frac{(3+\nu)\rho\omega^2 r_{ep}^2}{8} \tag{12}$$

Also, for the inner plastic zone $r \leq r_{ep}$ of the elastic plastic disc, the plastic stress distribution is given by Equation (7). Plastic stress distribution for $\omega = \omega_D$ are depicted in Figure 5 and Plastic/Elastic stress distribution for $\omega = \widetilde{\omega}_{SM}$ are depicted in Figure 6 where r_{ep} is defined by the vertical dash line.

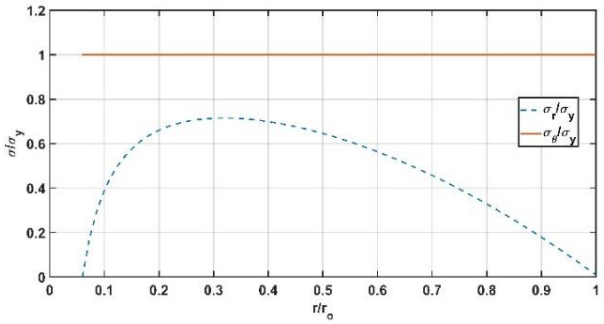

Figure 5: Normalised fully plastic stress distribution for design speed case

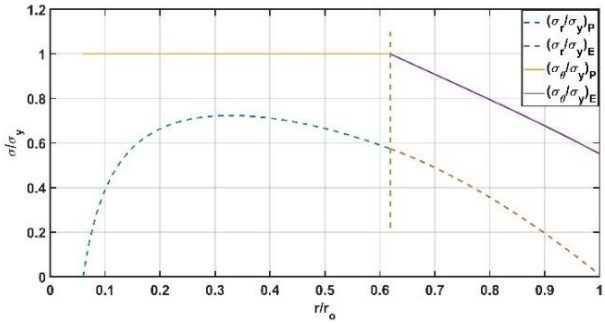

Figure 6: Normalised plastic to elastic stress distribution for operating speed case

4. Dynamic equation of Hy-FLY system

The dynamic equation of the system can be written as Equations (13), (14) and (15).

$$J_F\ddot{\theta}_F = T_F \tag{13}$$

$$J_M\ddot{\theta}_M = T_M \tag{14}$$

$$J_S\ddot{\theta}_S = T_S \tag{15}$$

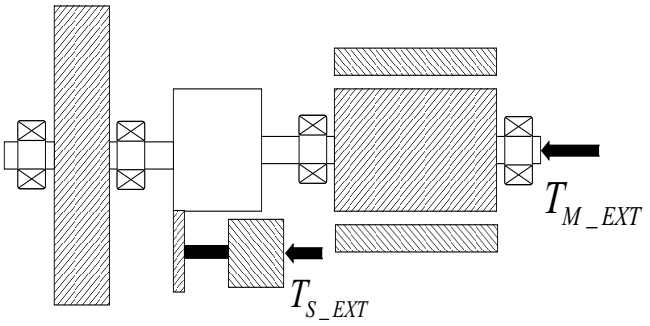

Figure 5: Shows the direction of the external torque acting on proposed system (Hy-FLY).

where T_F, T_M, T_S are the torques in the flywheel, synchronous machine, and secondary motor. T_F, T_M, and T_S have each two components as:

$$T_F = T_{F\_EXT} + T_{F\_CONSTRAINT} \tag{16}$$

$$T_M = T_{M\_EXT} + T_{M\_CONSTRAINT} \tag{17}$$

$$T_S = T_{S\_EXT} + T_{S\_CONSTRAINT} \tag{18}$$

The first component is the externally applied torque and the second component is the constraints part which comes into existence due to the inherent geometry of the epicyclic gears. There is no externally applied torque in the flywheel shaft in the Hy-FLY system. θ_F,θ_M, and $\theta_S$are the angular displacements of the flywheel, synchronous motor, and secondary motor shafts. The angular velocities of the flywheel, synchronous motor, and secondary motor shafts are related the angular displacements as:

$$\omega_F \triangleq \dot{\theta}_F,\ \omega_M \triangleq \dot{\theta}_M, \text{ and } \omega_S \triangleq \dot{\theta}_S$$

The angular displacements of planetary gears are constrained as follows:

$$[p \quad q \quad r]\begin{bmatrix}\theta_F\\ \theta_M\\ \theta_S\end{bmatrix} = 0 \tag{19}$$

where p, q, and r are the scalar quantities and the number of teeth in the planetary gears determines these values. The three angular displacements can be written in terms of two angular velocities using a transformation matrix as:

$$\begin{bmatrix}\theta_F\\ \theta_M\\ \theta_S\end{bmatrix} = \boldsymbol{T}\begin{bmatrix}\theta_M\\ \theta_S\end{bmatrix} \tag{20}$$

The constraints part of the torques do not contribute to work

and hence, $$\boldsymbol{T}^T\begin{bmatrix}T_{F\_CONSTRAINT}\\ T_{M\_CONSTRAINT}\\ T_{S\_CONSTRAINT}\end{bmatrix} = 0 \tag{21}$$

Using equation (20), equations (13), (14) and (15) can be reduced to the following equation

$$\begin{bmatrix}\frac{q^2}{p^2}J_F + J_M & \frac{qr}{p^2}J_F\\ \frac{qr}{p^2}J_F & \frac{r^2}{p^2}J_F + J_S\end{bmatrix}\begin{bmatrix}\ddot{\theta}_M\\ \ddot{\theta}_S\end{bmatrix} = \begin{bmatrix}T_{M\_EXT}\\ T_{S\_EXT}\end{bmatrix} \tag{22}$$

The frequency of the grid fluctuates whenever there is a mismatch between the generation and demand power. The frequency of the grid rises when generated power is more than the demand and the frequency decreases when demand is more than the generated power. For a stable operation of the grid a balance between the demand and generation must be maintained, so that, the grid frequency is maintained in an acceptable range. For the Indian grid, the acceptable range is 49.5-50.5 Hz. A negative load torque acts on the synchronous generator when the demand is more than the generation. This torque is proportional to the difference between the generation and demand power and also the *sine* of the load angle where the load angle (sometimes also called torque angle) is defined as the angle between the MMF of the rotor and the resultant MMF. This load torque tries to slow down the rotational speed of the synchronous generator, whose speed determines the frequency of the grid. Similarly, when demand is less than the generation, a positive torque acts on the machine, which tries to increase the speed of the generator. The rate at which this generator changes its speed depends on the inertia of the generator given by the well-known swing equation. The Hy-FLY system is connected to the grid and rotates synchronously to the grid frequency. An imbalance in the grid is instantly addressed by the high inertia of the flywheel of Hy-FLY, which arrests the rate of change of frequency by its high inertia while the frequency is stabilized by injecting or receiving the power from the grid.

In case of loss of generation, the electromechanical DDU applies a negative torque to the flywheel and to the secondary motor rotor by maintaining a positive torque equal to the load torque to the primary synchronous machine rotor. The secondary motor is powered by the secondary energy storage. The electromechanical DDU draws power from the flywheel and the secondary energy storage simultaneously to power the primary synchronous machine.

In case of loss of demand, the electromechanical DDU applies a positive torque to the flywheel and to the secondary motor rotor by maintaining a negative torque equal to the load torque to the primary synchronous machine rotor. The electromechanical DDU draws power from the grid and stored in the flywheel and the secondary energy storage simultaneously.

The DDU allows a slip between the speed of the flywheel and the speed of the primary synchronous machine while operating in the different modes that allows the flywheel to spins at different speeds while a constant speed of the primary synchronous machine is maintained.

A close loop control system is used, which works on the difference between the speed of the primary synchronous machine and the desired speed. For a 2-pole synchronous machine the desired speed is 100π. The torque on the secondary synchronous machine powered by the secondary

energy store is controlled in order to maintain a constant torque on the primary synchronous machine.

5. Conclusion and future work

The rapid integration of renewable energy into the grid and replacement of system inertia associated with the traditional turbogenerators has created a need for a hybrid system that provides inertia to address the sudden imbalance in the grid and energy storage to address the intermittent nature of the renewable energy sources. The hybrid energy storage system (Hy-FLY) presented here combines two energy sources where a flywheel is added to address the sudden imbalance in the grid and secondary energy storage (compressed air energy storage) to address the prolonged energy requirement. The inherent high level of inertia, high turnaround efficiency, high cycle life, high energy density, and low environmental effect make the usage of flywheel energy storage advantageous. A 50 MW, 20 MWh flywheel-based energy system is proposed to be built with elastic-perfectly-plastic material according to the Tresca yield criterion. The primary aim of this manuscript is to introduce a hybrid energy storage system that uses an epicyclic gear-based electromechanical differential drive unit which enables the system to operate in different modes while extracting the energy from the multiple energy sources. Future research should aim to assess the possibility of design improvements.

References

[1] K. S. Ratnam, K. Palanisamy, and G. Yang, 'Future low-inertia power systems: Requirements, issues, and solutions - A review', *Renewable and Sustainable Energy Reviews*, vol. 124. Elsevier Ltd, May 01, 2020. doi: 10.1016/j.rser.2020.109773.

[2] E. M. Carlini, F. Del Pizzo, G. M. Giannuzzi, D. Lauria, F. Mottola, and C. Pisani, 'Online analysis and prediction of the inertia in power systems with renewable power generation based on a minimum variance harmonic finite impulse response filter', *International Journal of Electrical Power and Energy Systems*, vol. 131, Oct. 2021, doi: 10.1016/j.ijepes.2021.107042.

[3] F. D\'\iaz-González, A. Sumper, and O. Gomis-Bellmunt, *Energy storage in power systems*. John Wiley \& Sons, 2016.

[4] B. Sorensen, *Energy intermittency*. CRC Press, 2014.

[5] P. Jain, *Wind energy engineering*. McGraw-Hill Education, 2016.

[6] R. Pearmine, Y. H. Song, T. G. Williams, and A. Chebbo, 'Identification of a load--frequency characteristic for allocation of spinning reserves on the British electricity grid', *IEE Proceedings-Generation, Transmission and Distribution*, vol. 153, no. 6, pp. 633–638, 2006.

[7] G. Yao, Z. Lu, Y. Wang, M. Benbouzid, and L. Moreau, 'A virtual synchronous generator based hierarchical control scheme of distributed generation systems', *Energies (Basel)*, vol. 10, no. 12, p. 2049, 2017.

[8] Y. Hirase, K. Abe, K. Sugimoto, K. Sakimoto, H. Bevrani, and T. Ise, 'A novel control approach for virtual synchronous generators to suppress frequency and voltage fluctuations in microgrids', *Appl Energy*, vol. 210, pp. 699–710, 2018.

[9] A. Fathi, Q. Shafiee, and H. Bevrani, 'Robust frequency control of microgrids using an extended virtual synchronous generator', *IEEE Transactions on Power Systems*, vol. 33, no. 6, pp. 6289–6297, 2018.

[10] H. Bevrani, T. Ise, and Y. Miura, 'Virtual synchronous generators: A survey and new perspectives', *International Journal of Electrical Power \& Energy Systems*, vol. 54, pp. 244–254, 2014.

[11] M. Dreidy, H. Mokhlis, and S. Mekhilef, 'Inertia response and frequency control techniques for renewable energy sources: A review', *Renewable and sustainable energy reviews*, vol. 69, pp. 144–155, 2017.

[12] H. Chen, T. N. Cong, W. Yang, C. Tan, Y. Li, and Y. Ding, 'Progress in electrical energy storage system: A critical review', *Progress in natural science*, vol. 19, no. 3, pp. 291–312, 2009.

[13] F. Faraji, A. Majazi, K. Al-Haddad, and others, 'A comprehensive review of flywheel energy storage system technology', *Renewable and Sustainable Energy Reviews*, vol. 67, pp. 477–490, 2017.

[14] R. Cárdenas, R. Peña, M. Pérez, J. Clare, G. Asher, and P. Wheeler, 'Power smoothing using a flywheel driven by a switched reluctance machine', *IEEE Transactions on Industrial Electronics*, vol. 53, no. 4, pp. 1086–1093, 2006.

[15] C. Tang, X. Dai, and X. Jiang, 'Design of a flywheel energy storage system for wind power fluctuation suppression', *Vibroengineering Procedia*, vol. 5, pp. 89–94, 2015.

[16] S. Samineni, B. K. Johnson, H. L. Hess, and J. D. Law, 'Modeling and analysis of a flywheel energy storage system for voltage sag correction', *IEEE Trans Ind Appl*, vol. 42, no. 1, pp. 42–52, 2006.

[17] J. P. Rouse, S. D. Garvey, B. Cárdenas, and T. R. Davenne, 'A series hybrid "real inertia" energy storage system', *J Energy Storage*, vol. 20, pp. 1–15, 2018.

[18] G. N. Prodromidis and F. A. Coutelieris, ‘Simulations of economical and technical feasibility of battery and flywheel hybrid energy storage systems in autonomous projects’, *Renew Energy*, vol. 39, no. 1, pp. 149–153, Mar. 2012, doi: 10.1016/j.renene.2011.07.041.

[19] R. Sebastián and R. Peña-Alzola, ‘Control and simulation of a flywheel energy storage for a wind diesel power system’, *International Journal of Electrical Power and Energy Systems*, vol. 64, pp. 1049–1056, 2015, doi: 10.1016/j.ijepes.2014.08.017.

[20] C. Carrillo, A. Feijóo, and J. Cidrás, ‘Comparative study of flywheel systems in an isolated wind plant’, *Renew Energy*, vol. 34, no. 3, pp. 890–898, Mar. 2009, doi: 10.1016/j.renene.2008.06.003.

[21] T. Bocklisch, ‘Hybrid energy storage systems for renewable energy applications’, in *Energy Procedia*, Elsevier Ltd, 2015, pp. 103–111. doi: 10.1016/j.egypro.2015.07.582.

[22] S. Ould Amrouche, D. Rekioua, T. Rekioua, and S. Bacha, ‘Overview of energy storage in renewable energy systems’, *Int J Hydrogen Energy*, vol. 41, no. 45, pp. 20914–20927, Dec. 2016, doi: 10.1016/j.ijhydene.2016.06.243.

[23] G. Shankar and V. Mukherjee, ‘Load frequency control of an autonomous hybrid power system by quasi-oppositional harmony search algorithm’, *International Journal of Electrical Power and Energy Systems*, vol. 78, pp. 715–734, Jun. 2016, doi: 10.1016/j.ijepes.2015.11.091.

[24] R. Nath, A. S. Bakshi, S. Ravinder, S. R. Narasimhan, H. Jain, and S. C. Shrivastava, ‘Report of the Expert Group: Review of Indian Electricity Grid Code’, *Community Emergency Response Team: New Delhi, India*, 2020.

[25] S. Hameer and J. L. van Niekerk, ‘A review of large-scale electrical energy storage’, *Int J Energy Res*, vol. 39, no. 9, pp. 1179–1195, 2015.

[26] J. W. Zhang, Y. H. Wang, G. C. Liu, and G. Z. Tian, ‘A review of control strategies for flywheel energy storage system and a case study with matrix converter’, *Energy Reports*, vol. 8, pp. 3948–3963, 2022.

[27] A. Nadai and L. H. Donnell, ‘Stress distribution in rotating discs of ductile material after the yield point has been reached’, *Trans. ASME*, vol. 51, no. pt I, pp. 173–180, 1929.

[28] A. Nadai, *Theory of Flow and Fracture of Solids; Volume 2*. New York, NY, McGraw-Hill Book Company Incorporated, 1963.

[29] D. W. A. Rees, *Mechanics of solids and structures*. World Scientific Publishing Company, 2016.

[30] ‘RoyMech;. Available from: https://www.roymech.co.uk/Useful_Tables/Matter/Strength_st.htm.’

[31] S. Timoshenko and J. N. Goodier, *Theory of Elasticity: By S. Timoshenko and JN Goodier*. McGraw-Hill, 1951.